SECTION C

UNRAVELLING A COMPLEX METAMORPHIC HISTORY USING PHASE-STABILITY MODELLING: METASOMATISM AND TRANSIENT THERMAL HETEROGENEITIES IN THE SALMON HOLE BROOK AND GARNET HILL SYNCLINES, CENTRAL-WESTERN NEW HAMPSHIRE

ABSTRACT

A newly developed approach to garnet isopleth thermobarometry has been applied to the staurolite-grade Littleton Schist to estimate the *P-T* conditions through which the Salmon Hole Brook and Garnet Hill Synclines in central western New Hampshire passed during the Acadian Orogeny. Well-constrained *P-T* paths have been calculated from nine samples taken from the Salmon Hole Brook Syncline and the southern portion of the Garnet Hill Syncline. Pressure variations in these *P-T* paths correlate well between samples, but temperature changes do not. Additionally, the relative rates of heating versus burial vary markedly between samples. The differences in the *P-T* paths between samples are not controlled by a regional metamorphic gradient, but appear to be randomly distributed across the field area. This could reflect the greater influence of geologic error on calculated temperatures versus calculated pressures that may result from the lower diffusivity of Ca in garnet versus that of Fe, Mg and Mn. Alternatively, if geological error is not significant, the results imply the existence of transient thermal gradients of up to $100\,°Ckm^{-1}$ that existed over a length-scale of ~200m and a time-scale comparable to that of garnet growth during prograde metamorphism. Both of these conclusions place constraints upon the precision with which regional *P-T-t* paths can be determined, and calls into question the veracity of inferred tectonic mechanisms that are based on subtle changes in the relative rates of heating and burial taken from a small number of samples.

Additionally, two distinct styles of metasomatism have been recognised in the Garnet Hill Syncline: carbon loss in the southwest, adjacent to the contact with the Bethlehem Granodiorite; and calcium loss in the northeast. The Ca-metasomatism was recognised by apparent disequilibrium measured between garnet core and bulk rock compositions. This process has rendered garnet isopleth thermobarometry useless in this

region, as it occurred after garnet growth, and changed the bulk rock composition significantly from what it was when garnet was growing. The carbon loss has not affected isopleth thermobarometry.

1. INTRODUCTION

P-T paths calculated from metamorphic rocks are one of the primary lines of evidence used by geologists to develop models of orogenic dynamics. The relative rates of heating with respect to burial, and how those rates vary between adjacent areas are used to infer the crustal-scale processes responsible for metamorphism (e.g., England & Thompson, 1984; Spear et al., 2002). A great deal of research has attempted to correlate *P-T* paths to tectonic processes and orogeny in the New England Appalachians, USA (e.g., Tracy et al., 1976; Kohn et al., 1992; Florence et al., 1993; Spear et al., 2002). Additionally, many new techniques for extracting *P-T* information from rocks were developed there (Thompson, 1976; Tracy et al., 1976; Vance & Holland, 1993; Evans, 2004). Isopleth thermobarometry is a relatively new technique that calculates the *P-T* of equilibration between a mineral and the chemical system in which it is growing. It has been applied most commonly to garnet porphyroblasts displaying growth zoning. However, until the development of complimentary techniques that allow for the effects of crystal fractionation on the bulk-rock composition (e.g., Marmo et al., 2002; Evans, 2004), it has only been useful for obtaining estimates of the *P-T* of garnet nucleation (Vance & Mahar, 1998), rather than the full *P-T* history of garnet growth. This study applies isopleth thermobarometry in conjunction with a modified version of the fractionation estimation methods described by Evans (2004) to 13 samples of garnet-bearing schist from the Littleton Formation to obtain *P-T* paths from across the Salmon

Hole Brook and Garnet Hill Synclines, and to recognise any metasomatic events that have influenced the chemistry of the region.

2. GEOLOGY

2.1. Regional Geology

The geology of the New Hampshire Appalachians has been studied for well over 100 years. The detailed geological mapping undertaken in the first half of the 20th Century remains a highly relevant and useful database (Billings, 1937). The gross crustal architecture is the result of mid-late Devonian deformation accommodating the accretion of Avalon and related terranes from the southeast onto the Laurentian plate during the Acadian orogeny (Figure 1). Sediments from the Siluro-Devonian basins that separated Avalon and Laurentia and rocks from the Bronson Hill Magmatic Arc, an Ordovician island arc that lay submerged on the Laurentian margin during the Silurian and Devonian, have been extensively deformed, metamorphosed and intruded by granite as they were caught between the colliding continents. Rocks from the Bronson Hill Magmatic Arc now form the Bronson Hill anticlinorium, and are exposed as a series of domes extending from Connecticut to New Brunswick. Intrusion of the New Hampshire Plutonic Suite to the east of the Bronson Hill Anticlinorium accompanied Acadian metamorphism in central New Hampshire (Figure 2). The Bethlehem Granodiorite is regarded as the oldest member of the New Hampshire Plutonic Suite (Dorais, 2003), having intruded metasediments of the westernmost Central Maine Terrane early in the Acadian at 410±5Ma (Lyons et al., 1997). The Kinsman Quartz-Monzonite was emplaced at 413±5 (Barreiro & Aleinikoff, 1985) to the east of the Bethlehem Granodiorite. The Kinsman Quartz Monzonite is chemically very similar to the Bethlehem Granodiorite, and was probably derived from the same source, albeit one

that was more evolved, hotter and less hydrous (Thompson et al., 1968). It is less deformed than the Bethlehem Granodiorite, and in spite of the two being geochronologically indistinguishable, the Kinsman Quartz Monzonite is considered to have been emplaced after the Bethlehem Granodiorite based on the structural and chemical differences between the rocks (Dorais, 2003). This relative timing implies an eastward migration of plutonism during the Acadian in western New Hampshire.

There is continuing debate over the interpretation of the geology in the New Hampshire Appalachians; some current tectonic models proposed for the region are based on the classic models of Thompson et al. (1968), involving the transport and stacking of multiple thrust-nappes from the east to the west (e.g., Spear et al., 2002; Dorais, 2003). Other tectonic models propose the westward migration of a foreland basin and deformation front ahead of the advancing Avalon terrane (e.g., Bradley et al., 2000; Eusden et al., 2000). Deep seismic reflection profiling across southern New Hampshire (Ando et al., 1984) and across western Maine (Stewart, 1989) show prominent sub parallel reflectors that dip west at around 30˚ throughout the Bronson Hill Anticlinorium and the Central Maine Synclinorium. It is difficult rationalise the Thompson (1968) model in the light of this seismic data, and it is difficult to rationalise the Bradley et al. (2000) and Eusden et al. (2000) models in view of the eastward migration of plutonism in the region. The numerical modelling of Beaumont & Quinlan (1994) presents a compelling solution to the seismic reflector geometry across New Hampshire. They suggest that the Bronson Hill Anticlinorium and Central Maine Synclinorium are part of a distributed thrust belt in the prowedge of the Acadian Orogen. The observed geometry, kinematics and eastward migration of deformation within these regions supports their hypothesis. This topic is discussed further in Section D.

2.2. Geology of the Salmon Hole and Garnet Hill Synclines

2.2.1. Introduction

This region was first mapped by Billings (1937), and his work remains the basic geological resource for the area. Florence et al. (1993) conducted isograd mapping and detailed *P-T* work within the region, pioneering recently developed techniques in *P-T* path calculation. These workers developed a tectonic history based on the tectonic history proposed by Thompson (1968) and the modelling of Thompson & England (1984). They suggested that the Salmon Hole Brook and Garnet Hill synclines were hot thrust sheets that had been emplaced from the east, over the cooler basement rocks of the Orford-Piermont region. These interpretations are incompatible with the structure and kinematics of thrusting proposed herein. A new tectonic model for the region is developed in Section D. A geological map of the two synclines is presented in figure 3.

2.2.2. Structure

The Salmon Hole Brook and Garnet Hill synclines are located on the eastern flank of the Bronson Hill Anticlinorium. They are tight to isoclinal, plunge at ~30° towards 260°, overturned to the southeast, and separated by the northwest-dipping Northy Hill fault. The dominant matrix foliation is typically axial plane to the both synclines. However, a later, sub-horizontal crenulation cleavage with a consistent top-to-the-southeast shear-sense which overprints the subvertical axial plane cleavage is widely developed.

2.2.3. Metamorphism

The Garnet Hill and Salmon Hole Brook synclines are composed of a sequence of Silurian to Devonian metasediments that unconformably overly Ordovician felsic volcanics and metasediments. The Clough conglomerate is the basal unit to this sequence, but outcrops discontinuously around the synclines. The Silurian Fitch formation, a package of calcareous schist, calc-silicate and marble, overlies the Clough and occurs in thicknesses ranging from 7 to 600m (Billings, 1937). The Devonian Littleton formation, a package of pelitic, psammitic and carbonaceous schist and amphibolite overlies the Fitch formation and makes up the bulk of each syncline. It typically contains large, euhedral staurolite porphyroblasts (up to 10cm) and small (~2mm) euhedral garnets in a muscovite matrix with either biotite or chlorite. Chloritoid occurs locally in aluminous layers with garnet, biotite and chlorite, and locally staurolite.

The Bethlehem Granodiorite, a foliated sheet-like body that intrudes the southernmost tip of the Garnet Hill syncline, appears to have been emplaced along the Northy Hill fault. There is no change in metamorphic index minerals in the Littleton Formation adjacent to the Bethlehem Granodiorite; it contains garnet, staurolite and biotite throughout the Garnet Hill Syncline. However, there is a region around the contact with the Bethlehem Granodiorite that is highly depleted in carbonaceous material with respect to the rest of the Littleton Formation in the Garnet Hill and Salmon Hole Brook Synclines. The Northy Hill Fault truncates this depleted zone to the northwest, whilst its northeastern margin is diffuse. Large (~10mm diameter), inclusion-rich porphyroblasts of garnet and staurolite are characteristic of the Littleton Fm in the carbon-depleted zone, with the amount of carbonaceous material present increasing

steadily to the north (Appendix 7). Biotite is the dominant matrix mineral in this zone whereas muscovite and chlorite are dominant in the carbonaceous rocks.

3. METHODS

3.1. Thermobarometry

The intersecting isopleth method (Vance & Mahar, 1998; Marmo et al., 2002; Evans, 2004) was used exclusively to determine the *P-T* conditions of garnet growth. In this method THERMOCALC is used to calculate the *P-T* conditions of equilibration between garnet of a particular composition and the bulk composition of the rock in which it was growing. Garnet composition is measured by electron microprobe point-analysis, allowing the calculation of the *P-T* of equilibrium for very small volumes of garnet at specific locations within a porphyroblast. This means that the *P-T* history of garnet growth can be defined at a high spatial resolution. *P-T* paths for individual samples are generated using intersecting isopleths from a series of analyses from the core to the rim of several garnets. A modified version of the methods described in Evans (2004) is used, resulting in the calculation of a path through the *P-T* window in which the sample was growing garnet. The techniques described in Evans (2004) have been modified in two important ways:

1. The concept of the "reactive rim" has been dispensed with. This concept was hard to justify in the face of the fact that compositional zoning in garnet is so well preserved in the rocks used in this study. In the modified method, the most manganiferous garnet analysis is now assumed to be the earliest grown garnet. K_d values are calculated based on this assumption, from the equation:

$$K_d = \frac{3X_{Spss}}{8X_{Mn-bulk}}$$

Where X_{spss} is the molar proportion of spessartine in the most manganiferous garnet analysis, 3/8 X_{spss} is the molar proportion of MnO in garnet based on the formula for almandine-type garnet, $(Fe,Mg,Mn,Ca)_3Al_2Si_3O_{12}$, and $X_{Mn-bulk}$ is the molar proportion of Mn in the bulk rock composition.

2. A complete error analysis is now incorporated into the calculations, including propagation of analytical error, assessment of "geological error" (Worley & Powell, 2000), and calculation of the thermodynamic error. These various error types are separated so that their contributions towards the relative and absolute uncertainty of positions of points within the *P-T* path can be seen.

Figure 4 shows an example of the output of the modified technique, illustrating both the sources and the relative magnitudes of the different error contributions.

4. RESULTS

4.1. Petrological Modelling

All of the pseudosection and isopleth calculations are presented in Appendix 4. All of the spreadsheets used to generate the fractionation estimates used in the construction of the *P-T* paths are presented in Appendix 5. Appendix 2 shows backscattered electron images of most of the garnets analysed, with the analysis ID number and location marked.

4.1.1. DL-16 – garnet staurolite biotite muscovite plagioclase carbonaceous schist

The *P-T* pseudosection based on whole-rock XRF for this sample is shown in figure 5. Compositional isopleths based on the composition of the core of garnet were plotted on the pseudosection. All three of the core isopleths plotted within analytical error of each other, but run parallel and isothermally through the garnet-chlorite-

muscovite field. This sample was not considered suitable for *P-T* path modelling because of this.

4.1.2. DL-25 – garnet staurolite biotite muscovite plagioclase carbonaceous schist

The *P-T* pseudosection calculated using the whole-rock composition of DL-25 is presented in figure 6. Composition isopleths based on the core composition of garnet are plotted on the section. The almandine and spessartine isopleths plot as parallel lines that lie within analytical error of each other, whilst the grossular isopleth intersects them at ~9kbar within the garnet chlorite plagioclase muscovite field.

4.1.3. DL-30 – garnet staurolite biotite muscovite plagioclase carbonaceous schist

Figure 7a shows the *P-T* pseudosection for DL-30 with garnet core composition isopleths plotted. The compositional isopleths all intersect within the overlap of their 2σ analytical errors at 565°C and 5.1kbar, but the intersection is not as tight as in most of the other samples. Figure 7b shows the *P-T* progression of garnet compositional isopleth intersections from the core to the rim of garnet, calculated with respect to a fractionating bulk composition. Garnet in DL-30 grew during heating from 565°C to 575°C at ~5kbar. Any pressure change during garnet growth could not be resolved within the 95% confidence interval for the uncertainty in the compositional data.

4.1.4. DL-36 – chloritoid garnet staurolite biotite chlorite muscovite plagioclase carbonaceous schist

The pseudosection with garnet core isopleths plotted is shown in figure 8. Garnet core isopleths display a well-constrained intersection at 3kbar and 545°C within the garnet staurolite biotite chlorite field. *P-T* path calculations were not attempted

because of the disagreement between the stable core assemblage and the petrographic observations.

4.1.5. DL-38 – garnet staurolite biotite muscovite plagioclase non-carbonaceous schist

Figure 9a shows the *P-T* pseudosection and garnet core isopleths calculated for DL-38. The garnet core isopleths show a well-constrained intersection at 560˚C and 5.6kbar. Figure 9b shows the progression of garnet composition isopleths for the full range of garnet composition, calculated with respect to a fractionating bulk composition. Garnet in DL-38 grew during heating from 560˚ to 590˚C at 5.6kbar.

4.1.6. DL-44 – garnet biotite muscovite plagioclase carbonaceous schist

Figure 10a shows the *P-T* pseudosection and garnet core isopleths calculated for DL-44. Garnet core isopleths show a good intersection within the garnet-chlorite-plagiocalse-muscovite field. Figure 10b shows the *P-T* path derived from garnet's compositional range, calculated with respect to a fractionating effective bulk composition. Garnet in DL-44 grew during heating from 515 to 555˚C with compression from 5.0 to 5.6kbar.

4.1.7. DL-62 – garnet staurolite biotite muscovite plagioclase carbonaceous schist

Figure 11a shows the *P-T* pseudosection and garnet core isopleths calculated for DL-62. Garnet core isopleths intersect a significant distance within the garnet-chlorite-biotite-plagioclase field. Figure 11b shows the isopleth intersections from the core to the rim of a garnet in DL-62 calculated with respect to a fractionating effective bulk composition. Garnet in DL-62 grew during heating from 565 to 585˚C and

decompression from 5.5 to 5kbar. However, the decompression from core to rim is not resolvable at the 95% confidence interval.

4.1.8. DL-65 – garnet staurolite biotite muscovite plagioclase carbonaceous schist

Figure 12a shows the *P-T* pseudosection and garnet core isopleths calculated for DL-65. The core isopleths plot with a well-constrained intersection within the garnet chlorite plagioclase muscovite field. Figure 12b shows the *P-T* path calculated from this sample based on garnet compositional isopleth intersections calculated with respect to a fractionating effective bulk composition. Garnet grew during heating from 560 to 575˚C and decompression from 5.4 to 4.6kbar, although the decompression is not resolvable from core to rim within the 95% confidence interval.

4.1.9. DL-68 – garnet staurolite biotite muscovite plagioclase non-carbonaceous schist

Figure 13a shows the *P-T* pseudosection and garnet core isopleths calculated for DL-68. The core isopleths display a well-constrained intersection within the chlorite-plagioclase-biotite-garnet-muscovite field at 4.9kbar and 540˚C. Figure 13b shows the progression of garnet composition isopleths from core to rim, calculated to allow for crystal fractionation. The isopleths plot in a path that displays heating from 540 to 560˚C with burial from 4.9 to 5.4kbar, followed continued heating from 560 to 575˚C with decompression from 5.4 to 4.8kbar. The change in pressure and temperature from core to rim can be resolved within the 95% confidence interval for the analytical error on the garnet composition data.

4.1.10. TE19 – garnet staurolite biotite muscovite plagioclase carbonaceous schist

Figure 14a shows the *P-T* pseudosection and garnet core isopleths calculated for TE19. Garnet core composition isopleths display a well-constrained intersection within the garnet-staurolite-chlorite-plagioclase-muscovite field. Figure 14b shows the *P-T* path calculated for the core to rim compositions of garnet allowing for the effects of crystal fractionation on the bulk rock composition. The path displays heating from 545 to 560˚C with compression from 5.0 to 5.6kbar, followed by heating from 560 to 570˚C with decompression from 5.6 to 5.2kbar.

4.1.11. TE21 – garnet staurolite biotite chlorite muscovite plagioclase carbonaceous schist

Figure 15a shows the *P-T* pseudosection and garnet core isopleths calculated for TE21. The garnet core composition is in a well-constrained equilibrium with the bulk composition within the garnet-staurolite-plagioclase-chlorite-muscovite field. Figure 15b shows the *P-T* path calculated for the core to rim compositions of garnet allowing for the effects of crystal fractionation on the effective bulk composition. The path displays heating from 520 to 545˚C during compression from 4.8 to 5.6kbar, followed by heating from 545 to 555˚C during decompression from 5.6 to 5kbar.

4.1.12. TE35 – garnet staurolite biotite muscovite plagioclase carbonaceous schist

Figure 16a shows the *P-T* pseudosection and garnet core isopleths calculated for TE35. The garnet core isopleths display a well-constrained intersection within the garnet-chlorite-plagioclase-muscovite field. Figure 16b shows the *P-T* path calculated for the core to rim compositions of garnet allowing for the effects of crystal

fractionation on the effective bulk composition. The path displays heating from 555 to 585°C at 6kbar with no discernable change in pressure.

4.1.13. TE36 – chloritoid garnet biotite chlorite muscovite plagioclase carbonaceous schist

The *P-T* pseudosection for TE36 is shown in figure 17. Garnet core composition isopleths intersection could not be plotted because the highest possible value for spessartine content in the pseudosection was roughly four times lower than the values measured in garnet.

4.2. Summary of petrological modelling

Garnet growth in the Salmon Hole Brook Syncline and Garnet Hill Syncline occurred at 5-6kbar and from 520-590°C. The *P-T* paths are generally characterised by heating with a ~0.5kbar increase in pressure, followed by a pressure drop of ~0.5kbar (Figure 18). The peak temperature conditions of metamorphism are estimated to be <630°C as staurolite is the highest grade mineral recorded; neither sillimanite or kyanite were observed in any sample. The partial *P-T* paths obtained from garnet suggest a clockwise path, where peak pressure has preceded peak temperature.

The two samples from the north of the Garnet Hill Syncline (DL-16 and DL-25) all display distinct disequilibrium between garnet core and bulk rock compositions. Garnet from each of these samples displays normal prograde zoning and shows no signs of post-growth compositional alteration. Two samples from the south (DL-38 and DL-68) displaying evidence for carbon removal show good equilibrium relationships between the cores of garnet and the bulk compositions. Both of the chloritoid-bearing

samples used in this study (DL-36, TE36) have shown poorly constrained to non-existent equilibria between garnet core and bulk compositions.

5. DISCUSSION

5.1. *P-T* evolution

5.1.1. Local P-T paths

The most striking feature of the collection of *P-T* paths assembled here is the spread in temperature between samples. All of the samples have grown garnet within a well-constrained pressure window of 4.8-6.2kbar, showing compression at relatively lower temperatures, and decompression at higher temperatures; there is no apparent field gradient with respect to pressure. However, the temperature at which garnet nucleated varies by as much 50˚C between samples, and the temperature window over which garnet grew ranges from 20-40˚C. This highlights three key issues that complicate the correlation of temperature with time between samples:

1. The occurrence of non-contemporaneous garnet growth across the region.

2. The presence of thermal heterogeneity in the crust. That is, where a regionally significant temperature gradient, or a localised, transient temperature gradient exists at the time-scale of garnet growth.

3. Geological error impinging on calculated temperature, but not calculated pressure.

There does not appear to be a spatial control on the distribution of garnet core or rim temperatures. For example, TE21 and DL-65 are from adjacent outcrops, but the nucleation temperature for DL-65 is higher than the rim temperature for TE21. The *P-T* path recorded in DL-65 appears, based on the pressure decrease, to correlate with the latter part of the path recorded in TE21. This means that the two samples, separated by a

distance of 200m had a 20°C difference in temperature, which translates to a minimum estimate for a temperature gradient of 100°Ckm^{-1}. A thermal gradient of this magnitude must be highly transient over an orogenic time-scale (Stüwe, 2002), and could not have been maintained longer than the time-scale over which garnet growth occurred.

It is important to understand the mechanisms responsible for generating such a thermal regime if *P-T* path calculations are going to be used to generate a regional model for metamorphism. DL-65 is a quartz-rich rock with a small modal proportion of garnet, whilst TE21 is a very micaceous rock with a much higher modal proportion of garnet. The differences between these samples suggest two mechanisms by which the thermal gradient was established:

1. Garnet growth from chlorite breakdown is endothermic, so TE21 will potentially have been heated at a slower rate than DL-65 because it contains greater proportion of garnet and will have been more thermally influenced by that particular mineral reaction.

2. Garnet in both samples grew syn-tectonically. In the quartz-rich sample (DL-65), strain heating associated with plastically deforming quartz provided a significant thermal input. In the more micaceous sample (TE21), proportionally more of the deformation would have been accommodated by shear along mica cleavage, which should generate less strain heat.

The recognition of localised, transient thermal heterogeneity during metamorphism has important consequences for tectonic models drawn from *P-T* path calculations. It is crucial that *P-T* paths from a range of adjacent rocks are calculated to assess the magnitude of any local variation in the thermal history. Firstly, this allows limits to be set for the recognition of a significant regional gradient above the local thermal "noise". Secondly, it provides some uncertainty limits on the regional *P-T* path

and allows a more critical assessment of the tectonic models that are proposed to explain metamorphism.

5.1.2. The regional P-T path

No discernable difference between the *P-T* histories of the Garnet Hill Syncline and the Salmon Hole Brook Syncline stands out above the localised thermal heterogeneity measured in the areas. Garnet growth occurred along a gentle clockwise loop, commencing at between 4.8-6kbar (Figure 18). This implies that the synclines must have been buried to ~14-16km depth before they passed 520°C. These *P-T* conditions represent a significant up-temperature excursion from the stable continental geotherm, and suggest that the bulk of the burial occurred before the temperature breached the garnet zone, and that exhumation began prior to the cessation of heating. Florence et al. (1993) reported two occurrences of kyanite and one of andalusite in the north western Garnet Hill Syncline, but neither mineral was found in this study. The widespread occurrence of staurolite throughout both synclines, and the rarity of aluminosilicates provide an approximate upper limit on the region's peak metamorphic conditions (Figure 18).

5.3. Comparison with previous models

The P-T paths calculated in this study differ from those calculated by Florence et al. (1993) and Spear et al. (2002). These workers calculated paths that showed compression from 4 to 5.5kbar during heating from 530 to 570°C, which have a much faster rate of burial versus heating than the ones calculated in this study. They also showed isobaric cooling from the peak *P-T*. The method for calculating *P-T* paths used herein possesses significant advantages over the method used by Florence et al. (1993).

The method used by Florence et al. (1993) calculates the *P-T* of equilibration between garnet and zoned matrix plagioclase, assuming that garnet cores grew in equilibrium with plagioclase cores, and that garnet rims grew in equilibrium with plagioclase rims. In the absence of an empirical study comparing the compositions of zoned plagioclase in the matrix with plagioclase included in garnet, this assumption is unsupportable. Moreover, computer modelling of coexisting plagioclase and garnet composition and modal proportion illustrates that plagioclase is likely to be consumed during up-temperature garnet growth (Spear et al., 1991), casting significant uncertainty over any correlations between matrix plagioclase and garnet compositions. The method used herein removes the uncertainty associated with correlating the compositions of two physically unrelated analyses, and additionally provides an assessment of the validity of all the assumptions made about equilibrium from the quality of the isopleth intersections.

Another shortcoming of the Florence et al. (1993) method is the lack of any error propagation and analysis. The method used herein provides estimates of both the accuracy and the precision of the results, and requires an analysis of the relative contributions of the sources of those errors to determine the suitability of each sample for modelling. Finally, crystal fractionation resulting from garnet growth will have influenced the composition of all but the very earliest grown garnet cores (Hollister, 1966; Vance & Mahar, 1998; Evans, 2004). This process is not accounted for in the *P-T* path calculations used by Spear et al. (2002) and Florence et al. (1993), and would have significantly influenced the outcome of their calculations.

5.4. Metasomatism

The Garnet Hill Syncline underwent two distinct styles of metasomatism. Rocks from the south of the structure have undergone extensive removal of organic carbon, giving them a much lighter colour than the typical "mesozone" Littleton Formation common to the area. A likely cause of the removal of carbon from the rocks is that it was "burnt off" during the through-flow of oxidised fluid. The carbon-depleted zone is adjacent to the contact with the Bethlehem Granodiorite, suggesting that the oxidising fluids came from the cooling pluton. There is no evidence of any carbonaceous inclusions within garnet, staurolite or biotite porphyroblasts, suggesting that the metasomatism occurred prior to porphyroblast growth. This is consistent with the observations that the emplacement of the Bethlehem Granodiorite occurred early in the metamorphic history (Billings, 1937; Thompson & Norton, 1968). If this episode of metasomatism did predate garnet growth, then any changes other than carbon loss made to the bulk composition of the rock would not have affected isopleth thermobarometry results.

The two samples taken from the north of the Garnet Hill Syncline (DL-16 and D-25, Figures 5 and 6 respectively) display very poorly constrained garnet-core isopleth intersections. The non-intersection of the isopleths for these two samples appear to be caused by the Ca isopleth plotting at too high a pressure. An apparently elevated Ca isopleth is the result of garnet containing more Ca than it should, given the concentration of Ca in the bulk rock. This means that either garnet has had Ca added to it, or the bulk rock has had Ca removed from it following garnet growth. Given that garnet in both of these samples displays normal prograde zoning, it is unlikely its composition has been altered. Comparing the bulk composition analyses for all of the samples shows that there is no consistent difference between the three from the north of

the Garnet Hill Syncline and those from the rest of the area, other than the low Ca (Figure 19). Assuming that the low Ca values are not simply related to errors in the XRF analyses, they imply that Ca was not lost in conjunction with any other component, and that the metasomatism occurred at some time after garnet growth. Like the carbon loss in the south, the Ca-metasomatism is not present in the Salmon Hole Brook Syncline, implying that the Northy Hill Fault has either moved after the metasomatism occurred, truncating the metasomatised zones, or has moved before, and acted as a structural barrier to the flow of the metasomatic fluids, or both.

6. CONCLUSIONS

Metamorphism in the Salmon Hole Brook Syncline and the Garnet Hill Syncline is characterised by small-scale thermal gradients of up to $100°Ckm^{-1}$ over distances of ~200m. These gradients are not aligned to a regional metamorphic gradient, and are potentially a function of rock composition, being controlled by either strain and/or reaction enthalpy. No regional metamorphic gradient is apparent across the Salmon Hole Brook Syncline and Garnet Hill Syncline above the localised temperature variations, nor is there any difference in the *P-T* conditions of metamorphism between the two synclines. Both synclines were heated from ~520-550°C during compression from 4.8-6kbar and then were heated from ~550-590°C during decompression from 6-4.6kbar. The Garnet Hill Syncline has undergone two episodes of metasomatism. The earlier episode involved carbon loss in the south of the syncline and probably occurred before garnet growth. The latter metasomatic event resulted in the removal of Ca from rocks to the north of the Garnet Hill Syncline and occurred after garnet growth.

The success with chloritoid bearing samples using this method of *P-T* path determination was very limited (note poor to non-existent isopleth intersections in

chloritoid-bearing samples, figures 8 and 17). The reasons for this are not clear, but potentially relate to crystal fractionation associated with chloritoid growth, or with inaccurately described properties of chloritoid-bearing equilibria in the thermodynamic database.

UNRAVELLING A COMPLEX METAMORPHIC HISTORY USING PHASE-STABILITY MODELLING: METASOMATISM AND TRANSIENT THERMAL HETEROGENEITIES IN THE SALMON HOLE BROOK AND GARNET HILL SYNCLINES, CENTRAL-WESTERN NEW HAMPSHIRE
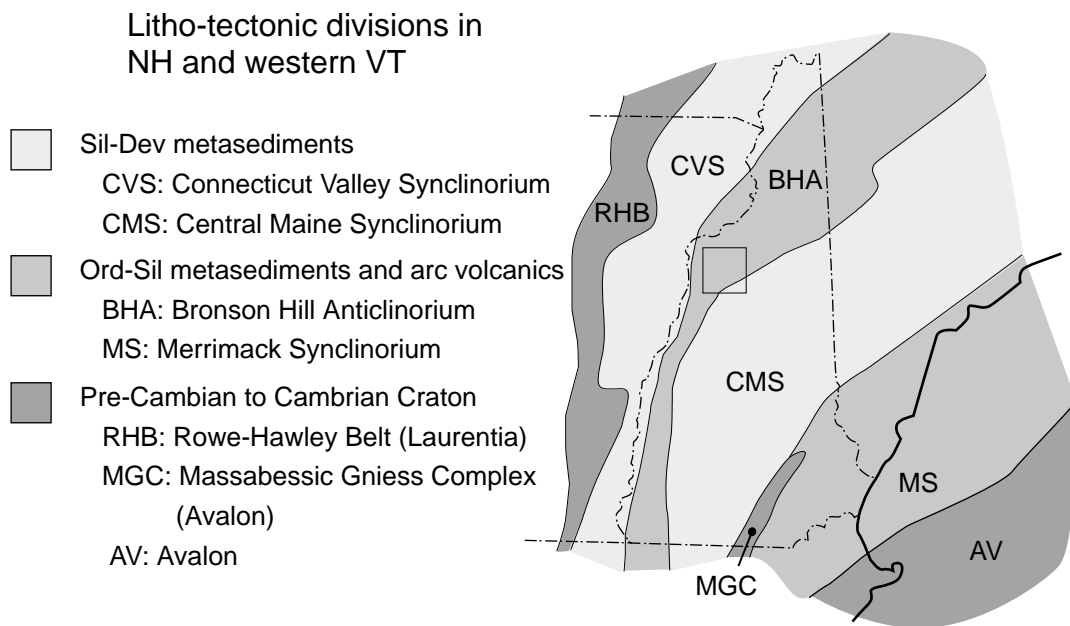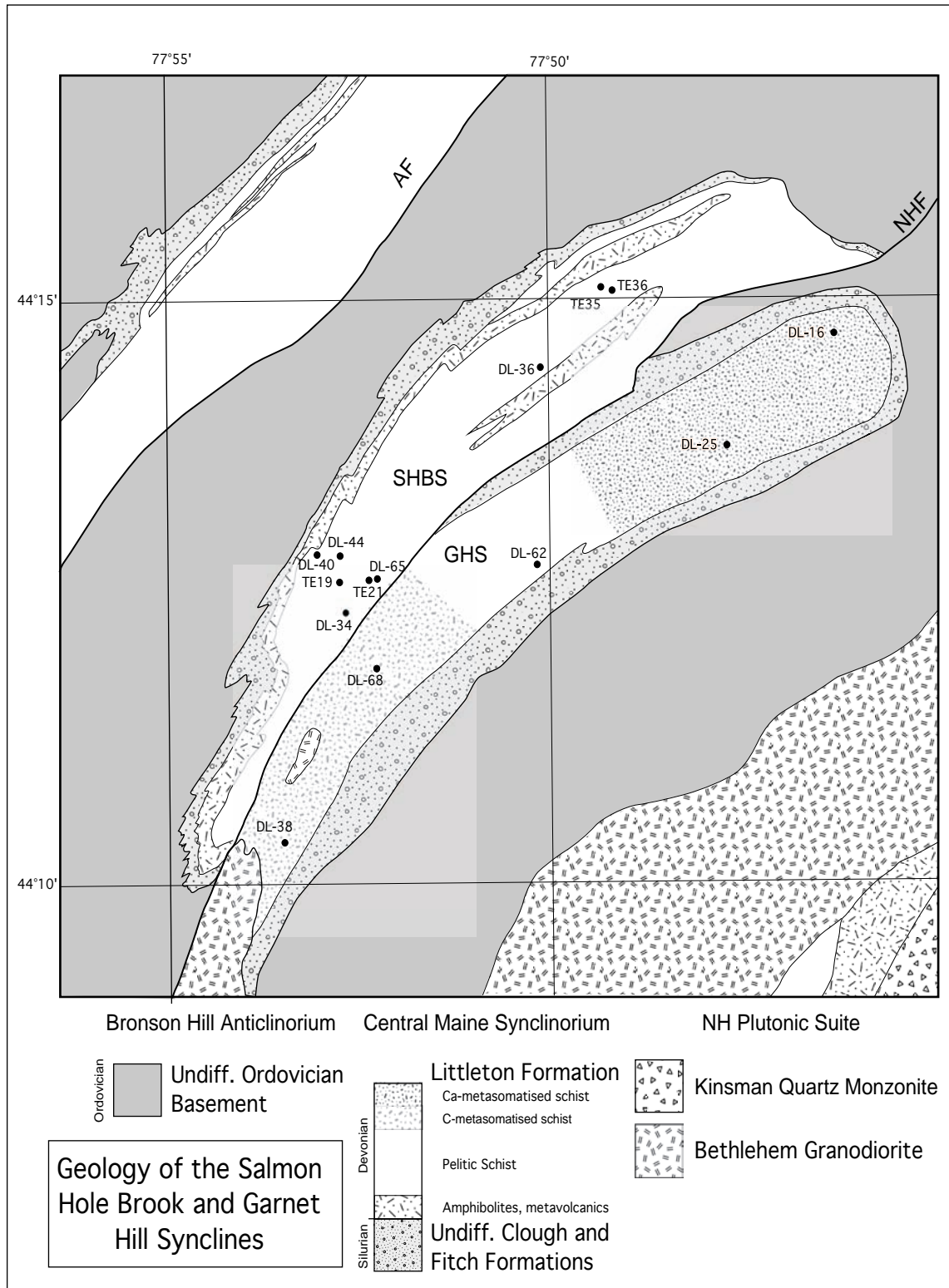
Figure 1. Generalised tectonic map of Vermont and New Hampshire.

The eastern flank of the Bronson Hill
Anticlinorium in central western NH
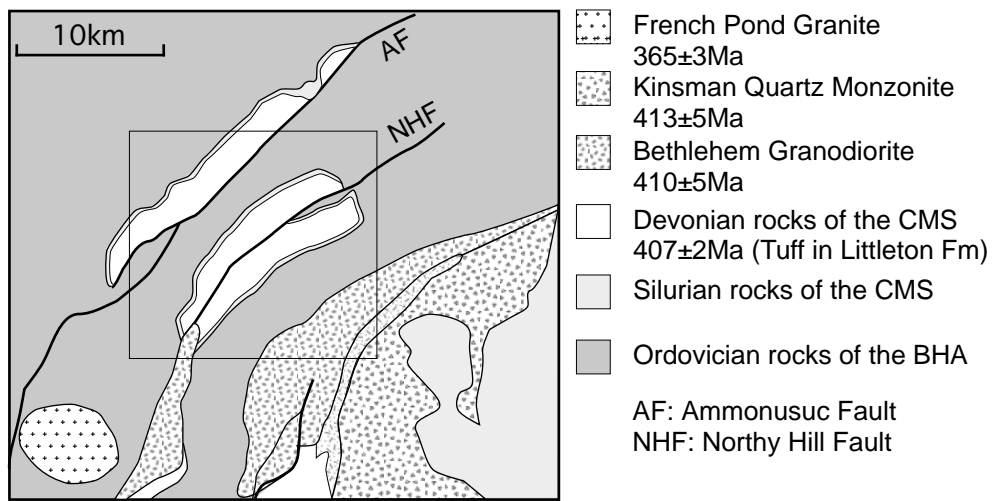
Figure 2. Geological map of the Littleton region.

Figure 3. Geological map of the Garnet Hill-Salmon Hole Brook synclines. Sample locations and the geographic extent of the two metasomatic events are shown. SHBS, Salmon Hole Brook Syncline; GHS, Garnet Hill syncline; NHF, Northy Hill Fault; AF, Ammonoosuc Fault.
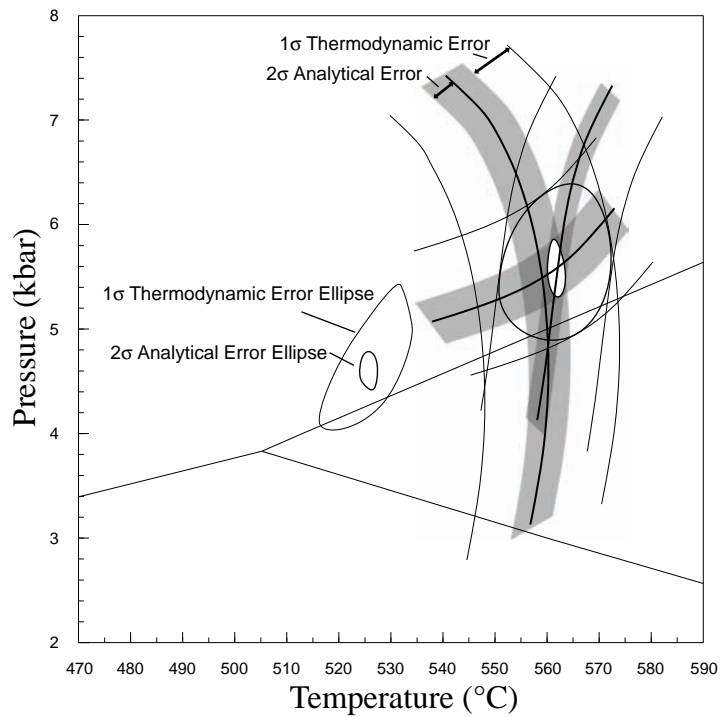
Figure 4. Calculated compositional isopleths for two garnet core from different samples showing the calculable systematic and random error contributions, and the ellipses used that represent the overlap of the different errors. The relative uncertainty in *P-T* position between the growth of these cores is represented by the black ellipses. The absolute accuracy of the calculations is represented by the unfilled ellipses. i.e., a *P-T* vector between the two black ellipses can only be absolutely constrained to within the confines of the unfilled ellipses at a 1σ confidence interval.

DL-16

MnNCKFMASH (+q mu H_2O)

Al_2O_3	CaO	MgO	FeO	K_2O	Na_2O	MnO
0.176	0.0018	0.0749	0.0836	0.0363	0.0147	0.00138

g chl

$X_{spss}=0.1427$

g st chl pl

g st bi pl

$X_{grss}=0.036$

$X_{alm}=0.7305$

chl pl

g chl pl

g sill bi pl
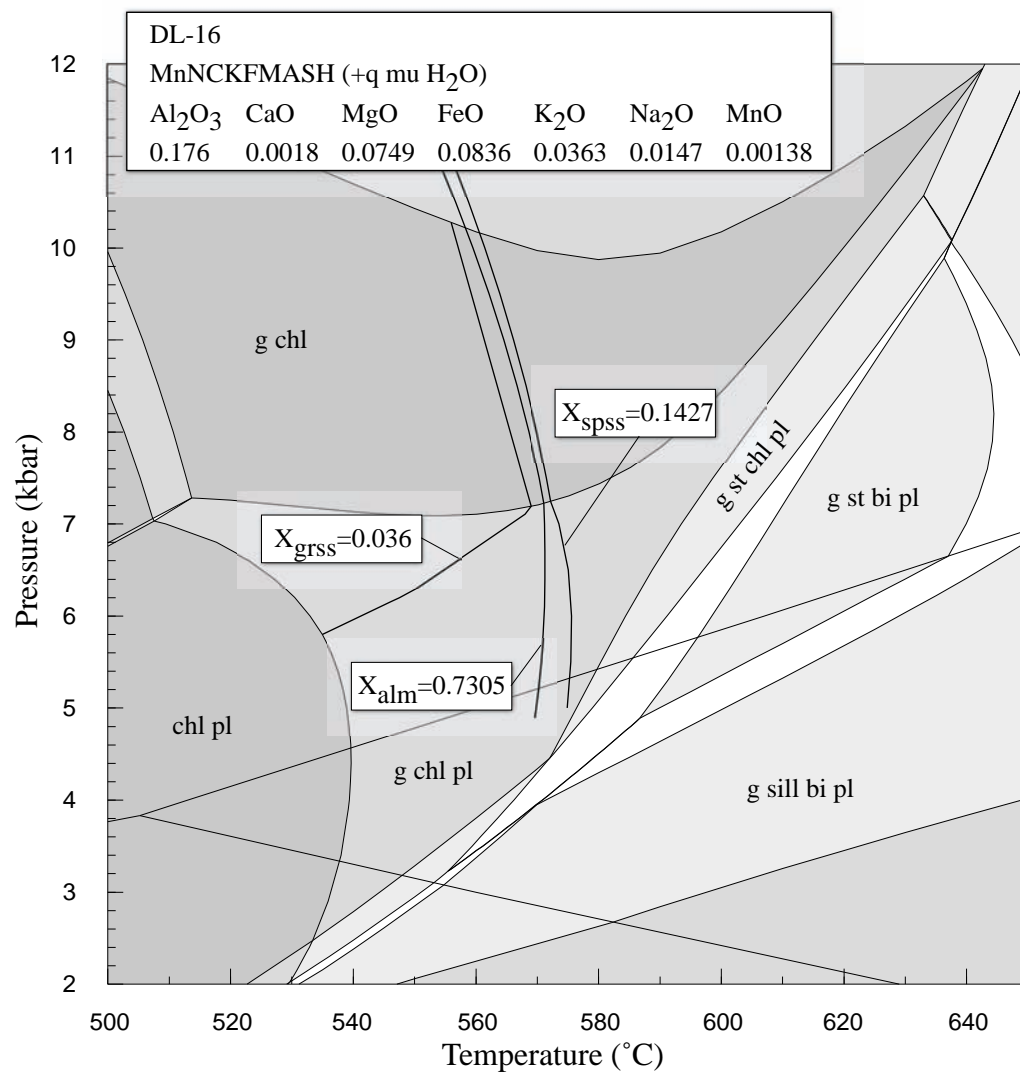
Figure 5. Pseudosection and garnet core isopleths for sample DL-16. The bulk composition and compositional isopleths are quoted as mol fractions.
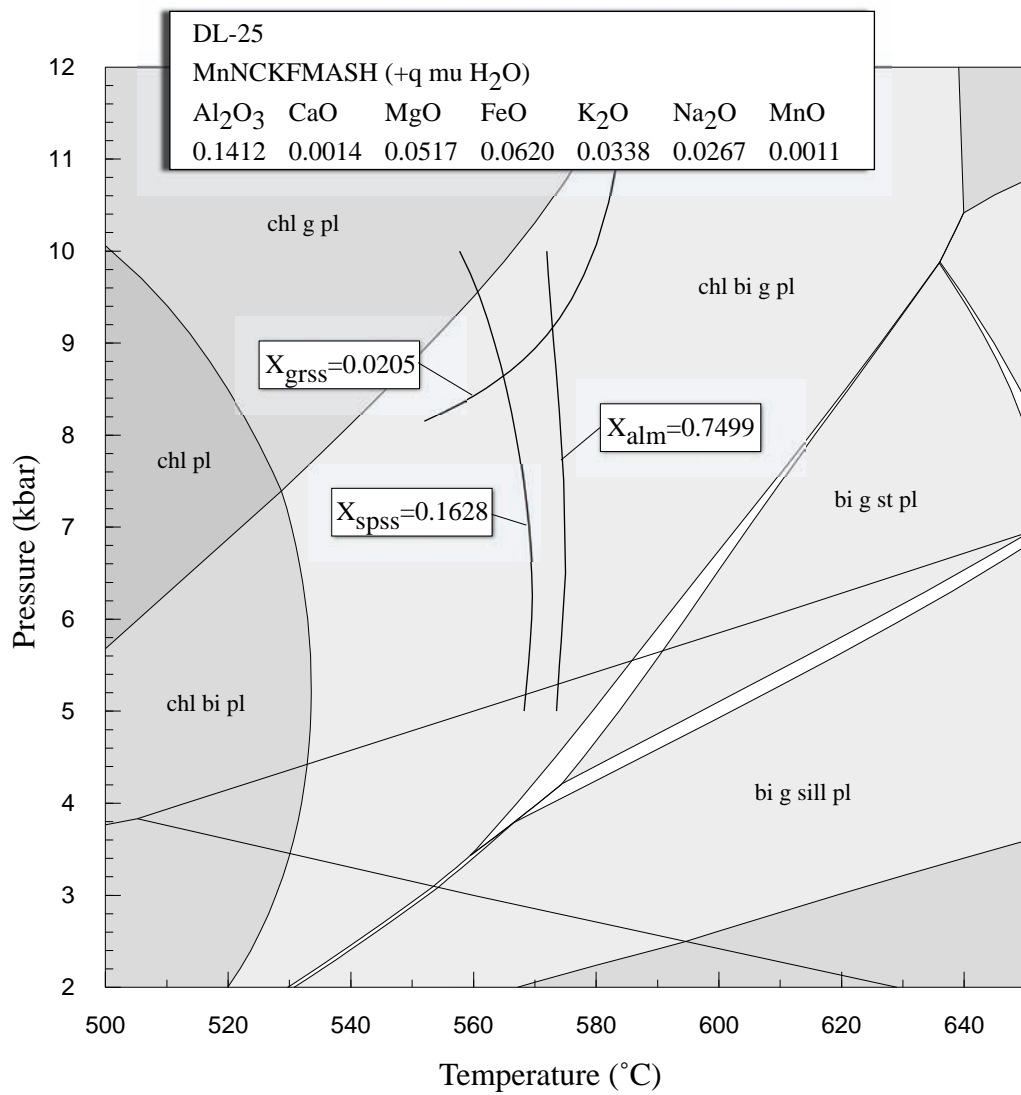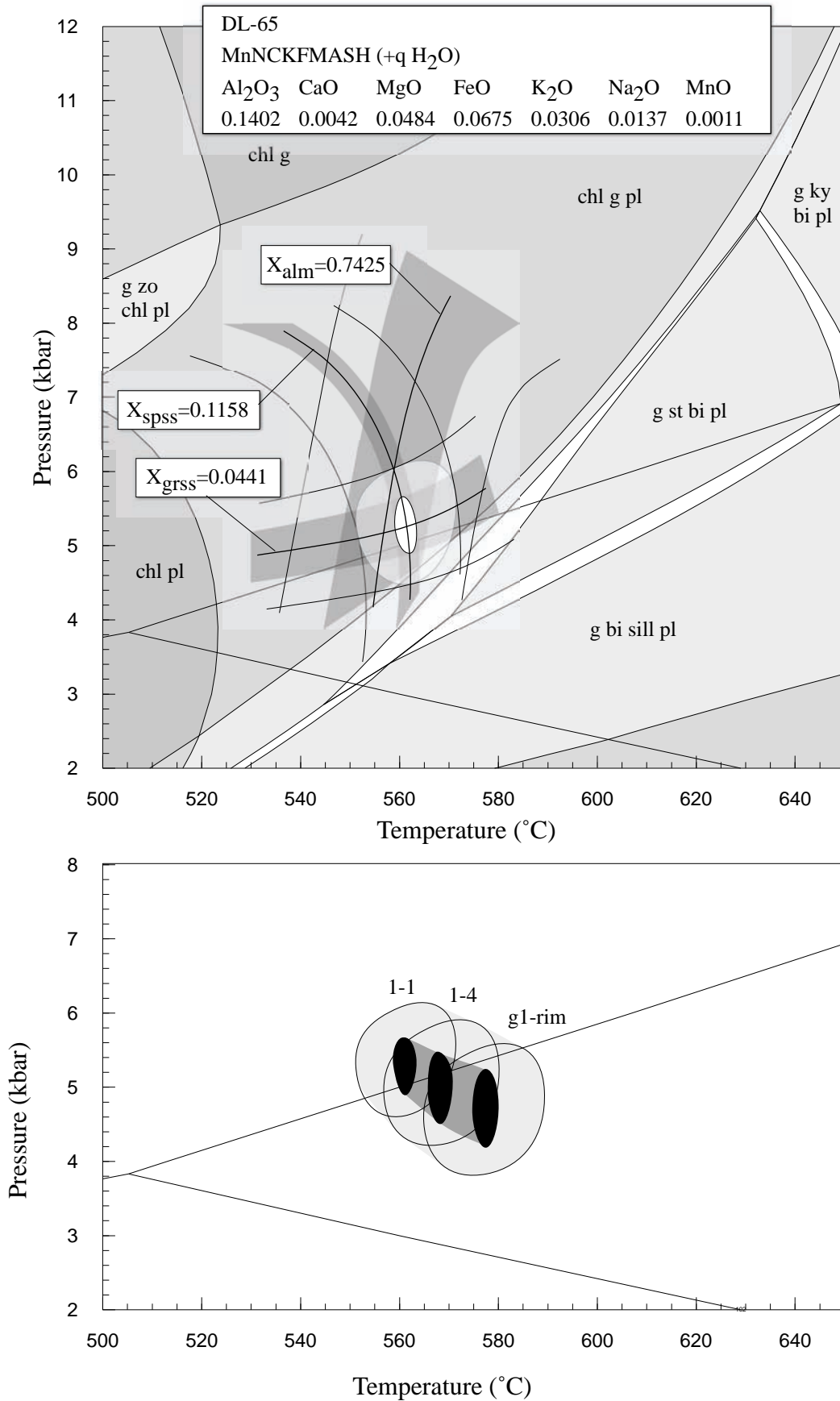
Figure 6. Pseudosection and garnet core isopleths for sample DL-25. The bulk composition and compositional isopleths are quoted as mol fractions.
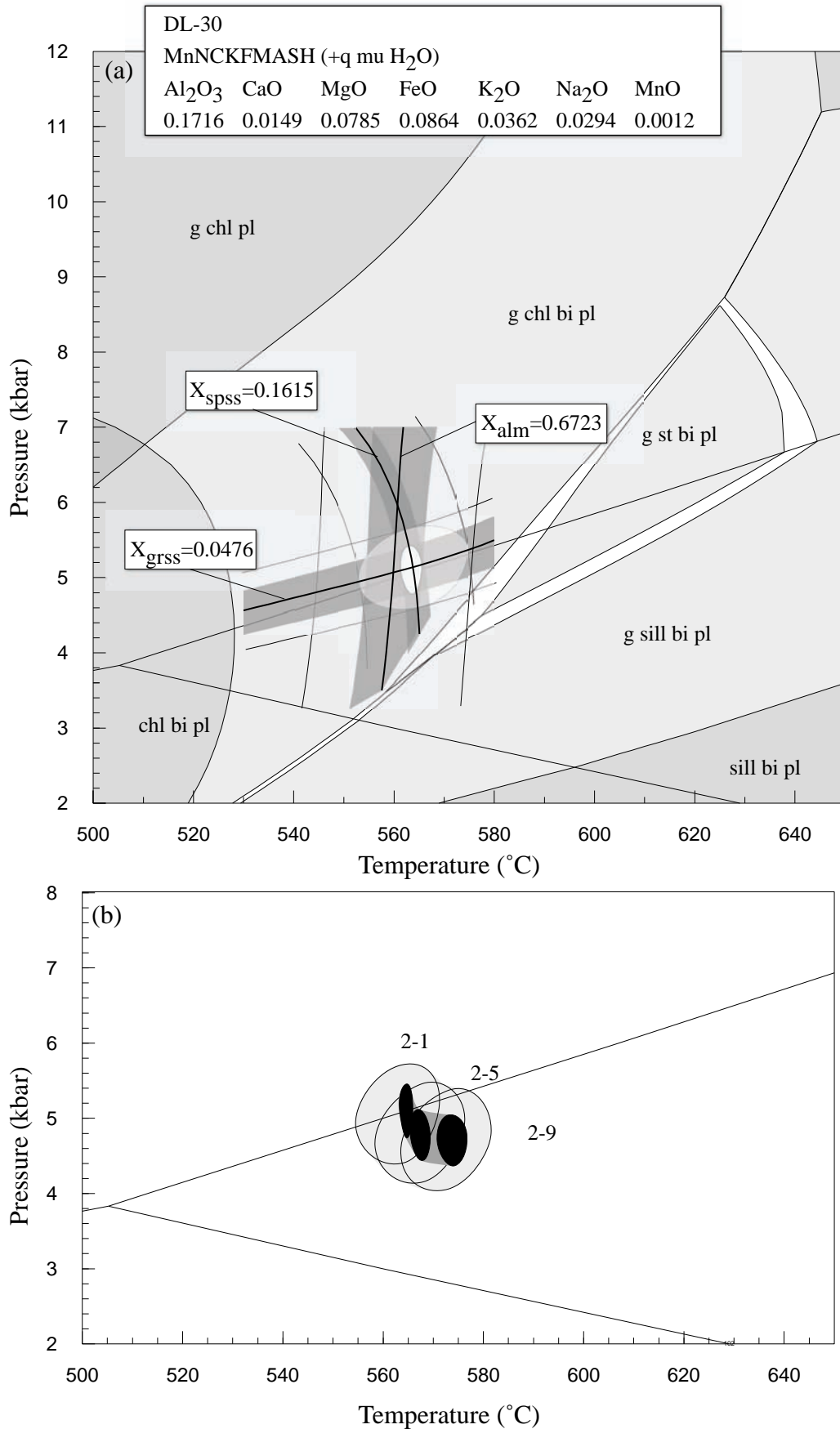
Figure 7. (a) Pseudosection and garnet core isopleths calculated for sample DL-30. **(b)** Core to rim isopleth intersection ellipses calculated with respect to a fractionating bulk composition. Numbers next to *P-T* points are the analysis ID. See Appendices 3-5.
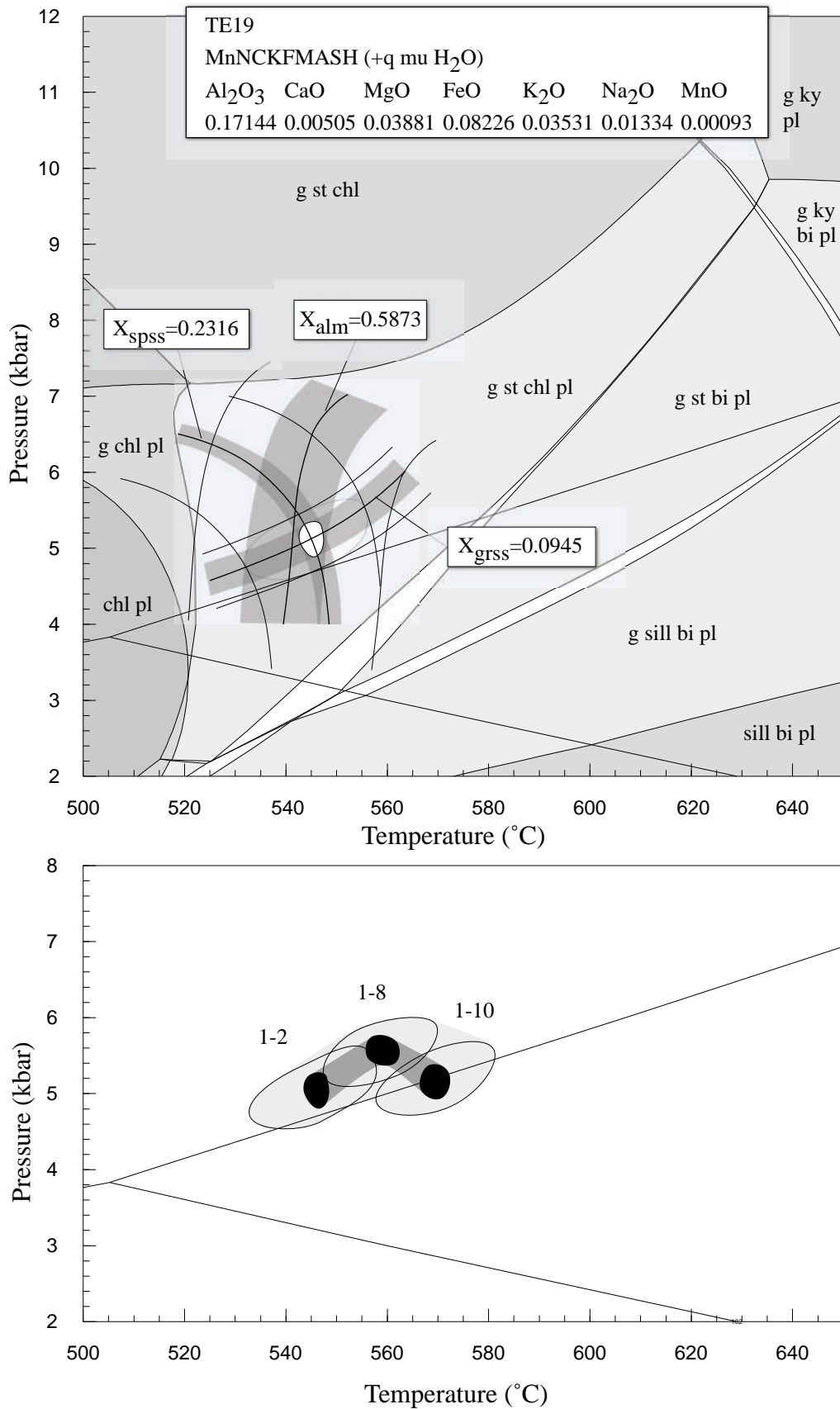
24
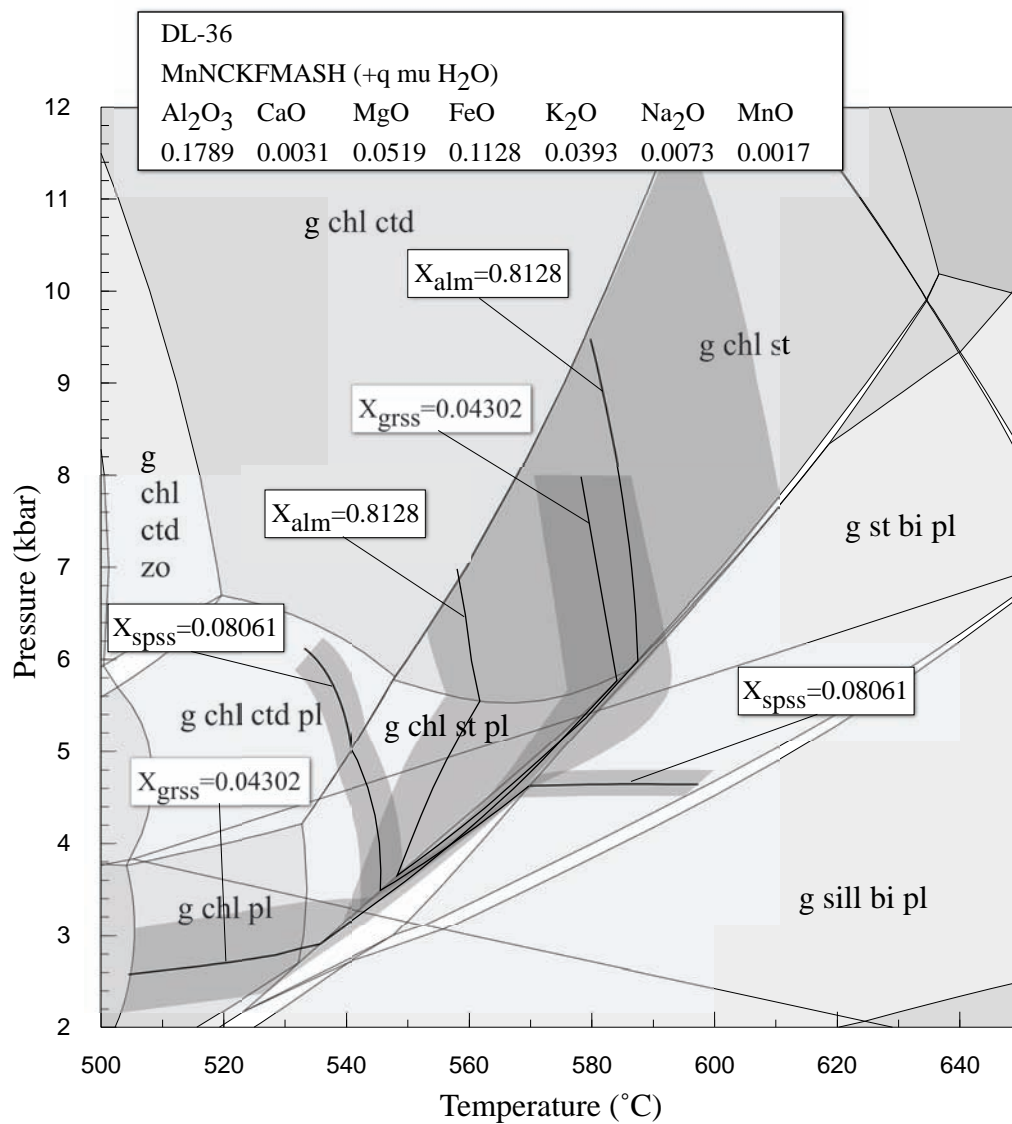
Figure 8. Pseudosection and garnet core isopleths for sample DL-36. The bulk composition and compositional isopleths are quoted as mol fractions.
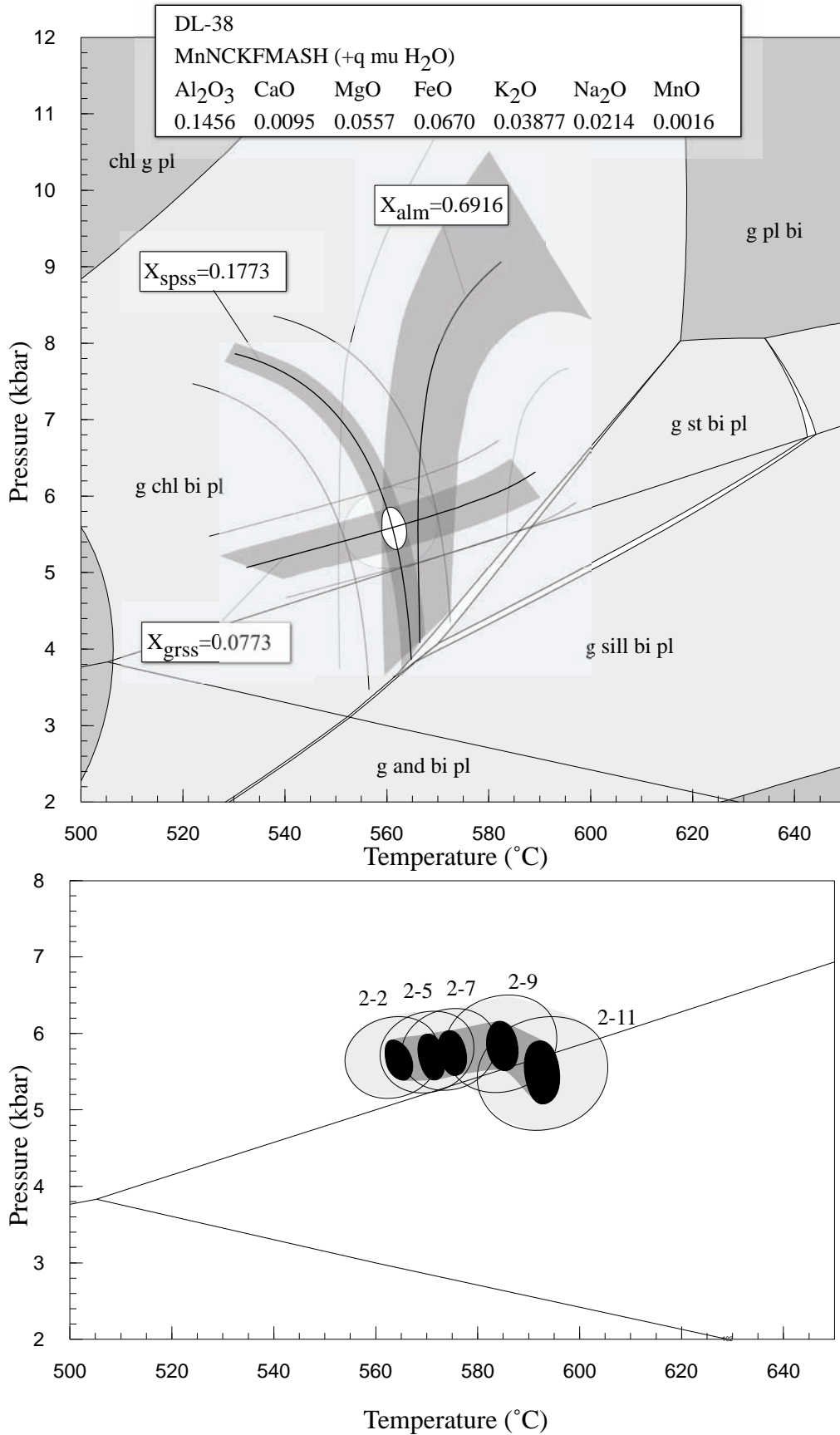
Figure 9. (a) Pseudosection and garnet core isopleths calculated for sample DL-38. **(b)** Core to rim isopleth intersection ellipses calculated with respect to a fractionating bulk composition
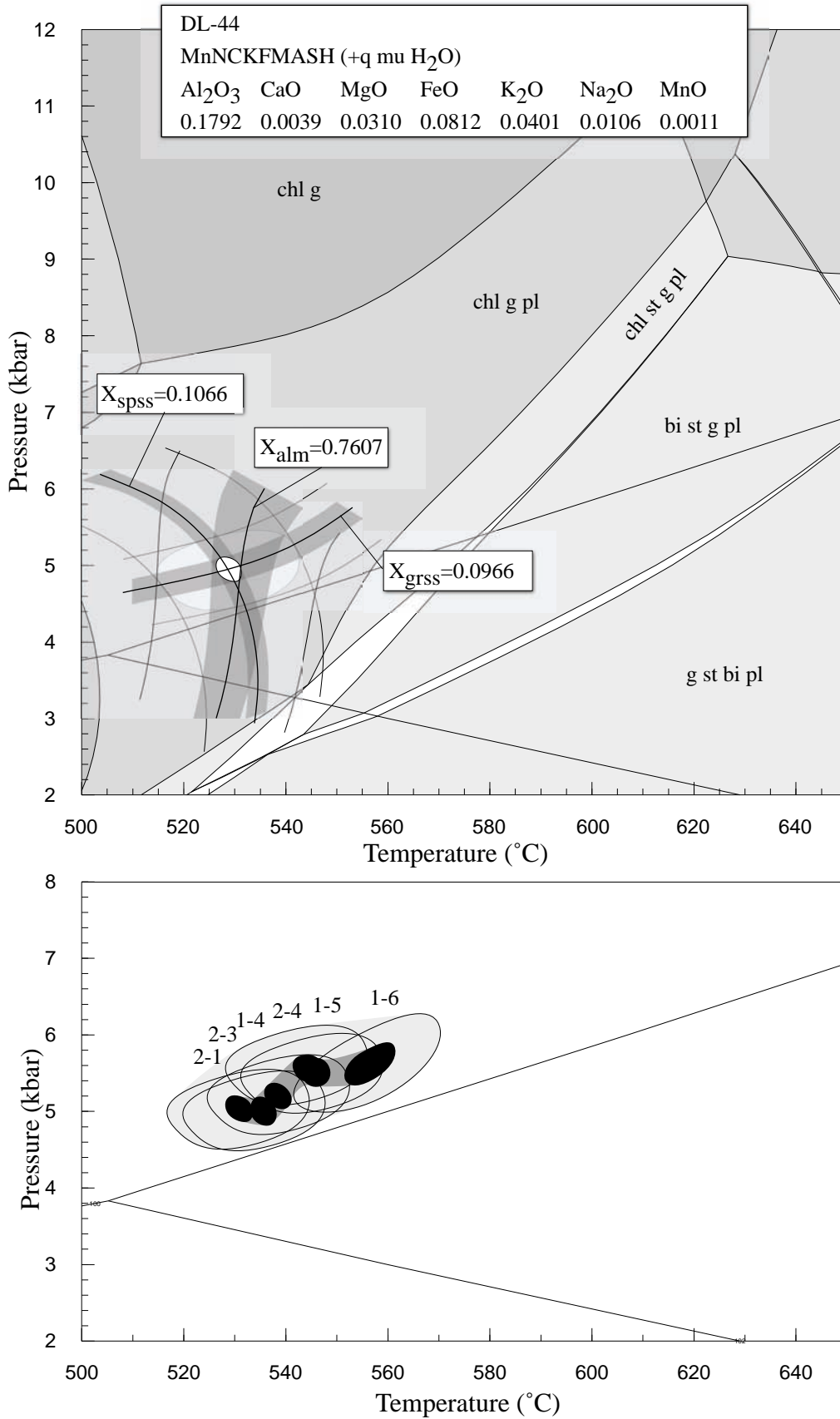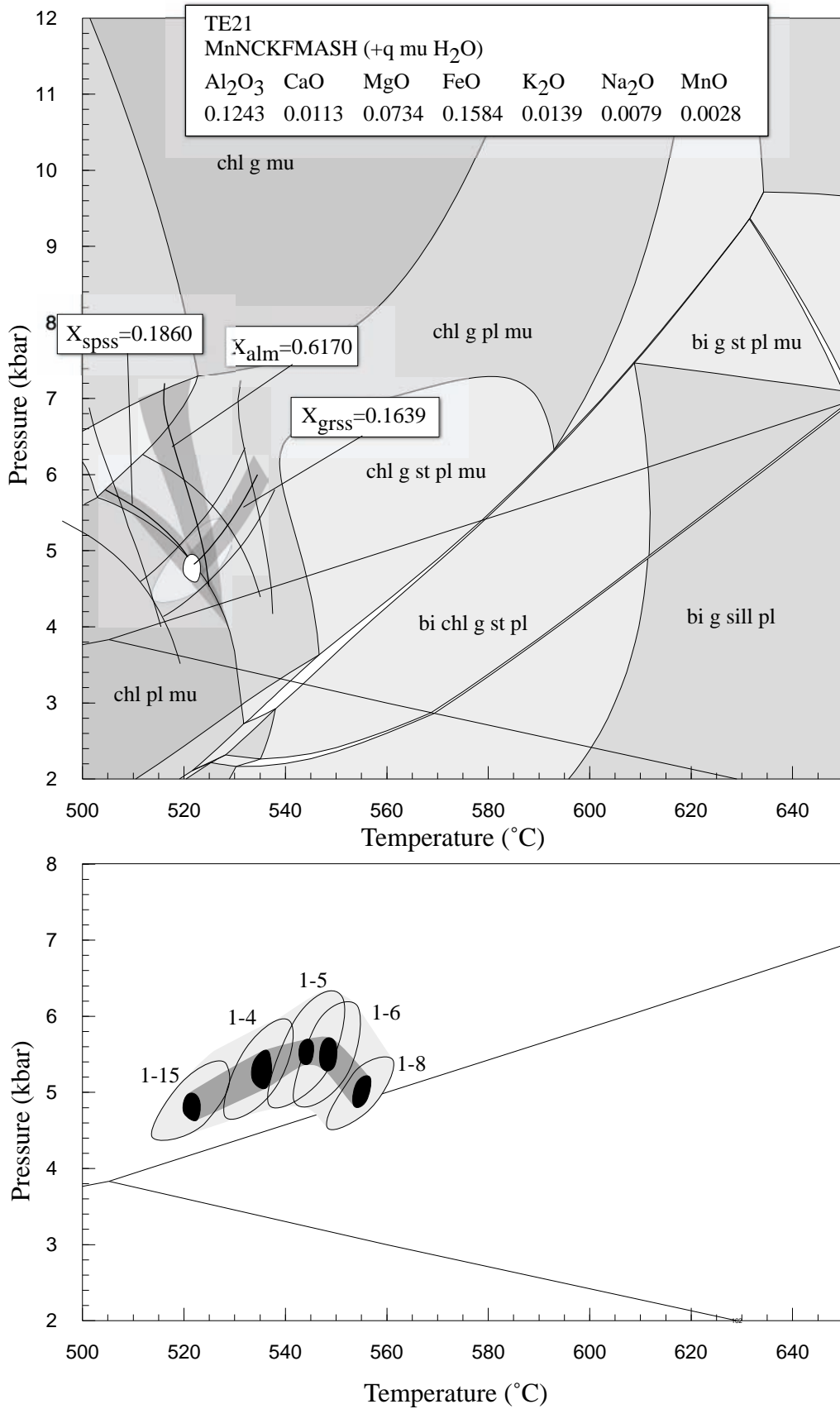
Figure 10. (a) Pseudosection and garnet core isopleths calculated for sample DL-44. **(b)** Core to rim isopleth intersection ellipses calculated with respect to a fractionating bulk composition
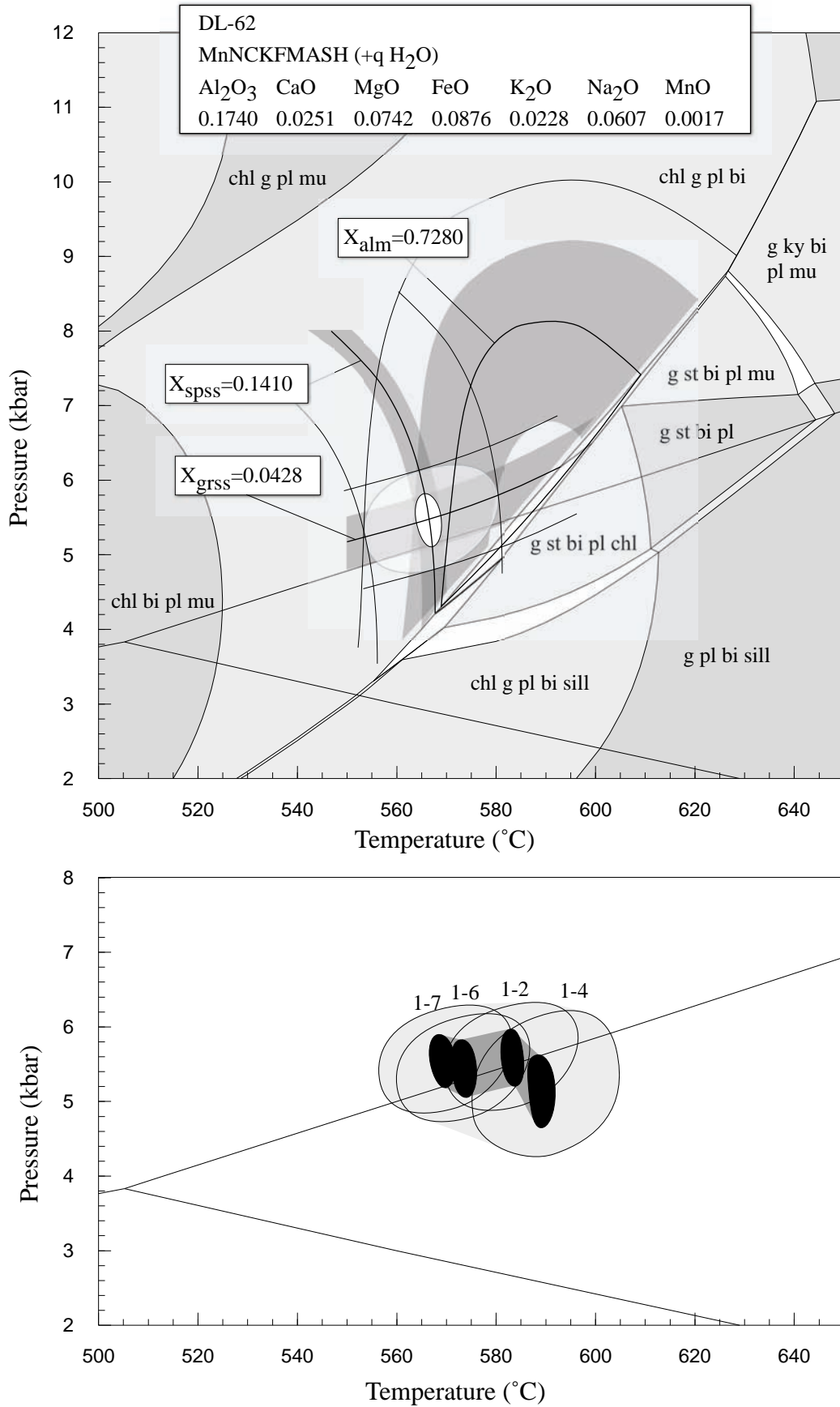
Figure 11. (a) Pseudosection and garnet core isopleths calculated for sample DL-62. **(b)** Core to rim isopleth intersection ellipses calculated with respect to a fractionating bulk composition
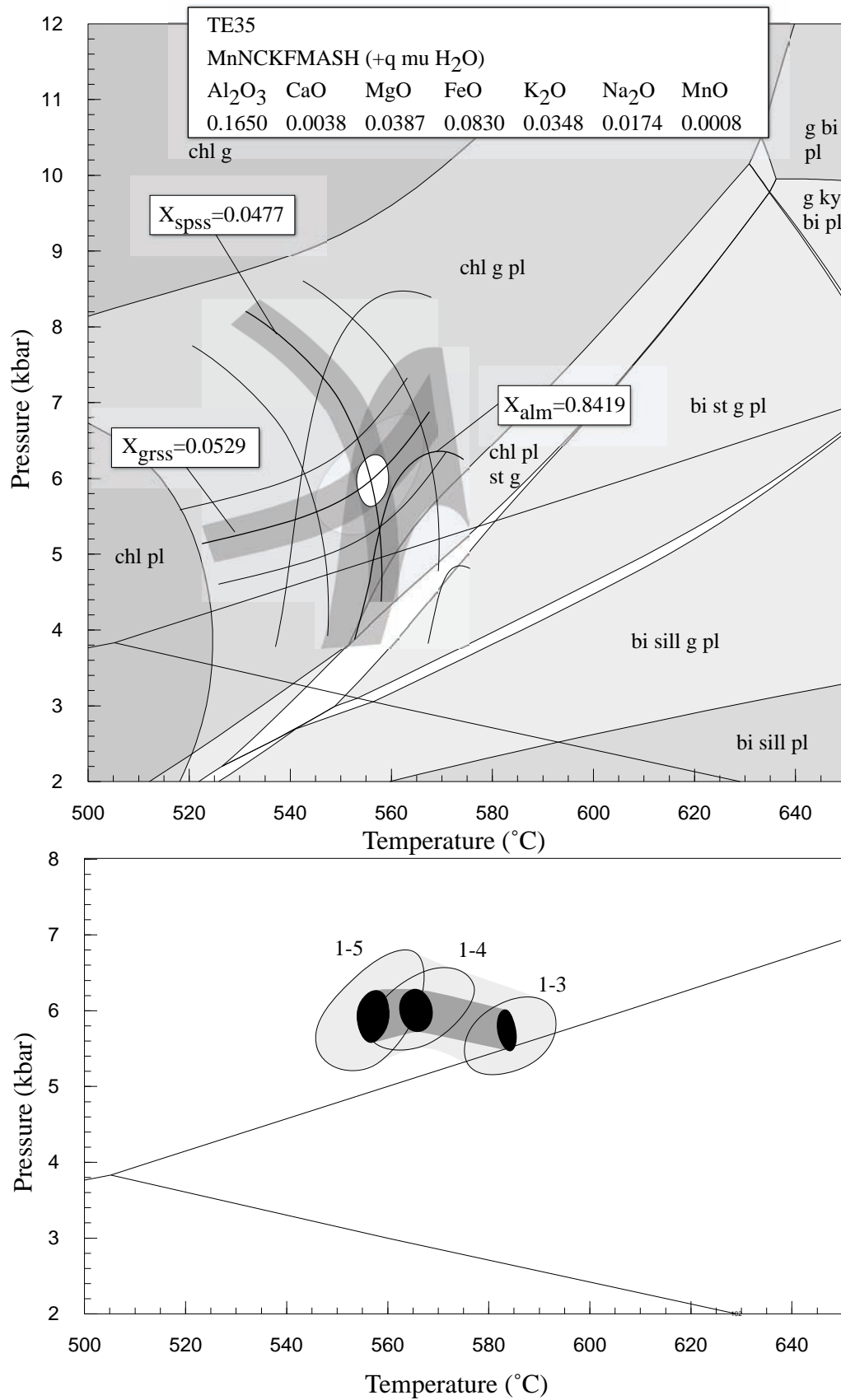
Figure 12. (a) Pseudosection and garnet core isopleths calculated for sample DL-65. **(b)** Core to rim isopleth intersection ellipses calculated with respect to a fractionating bulk composition
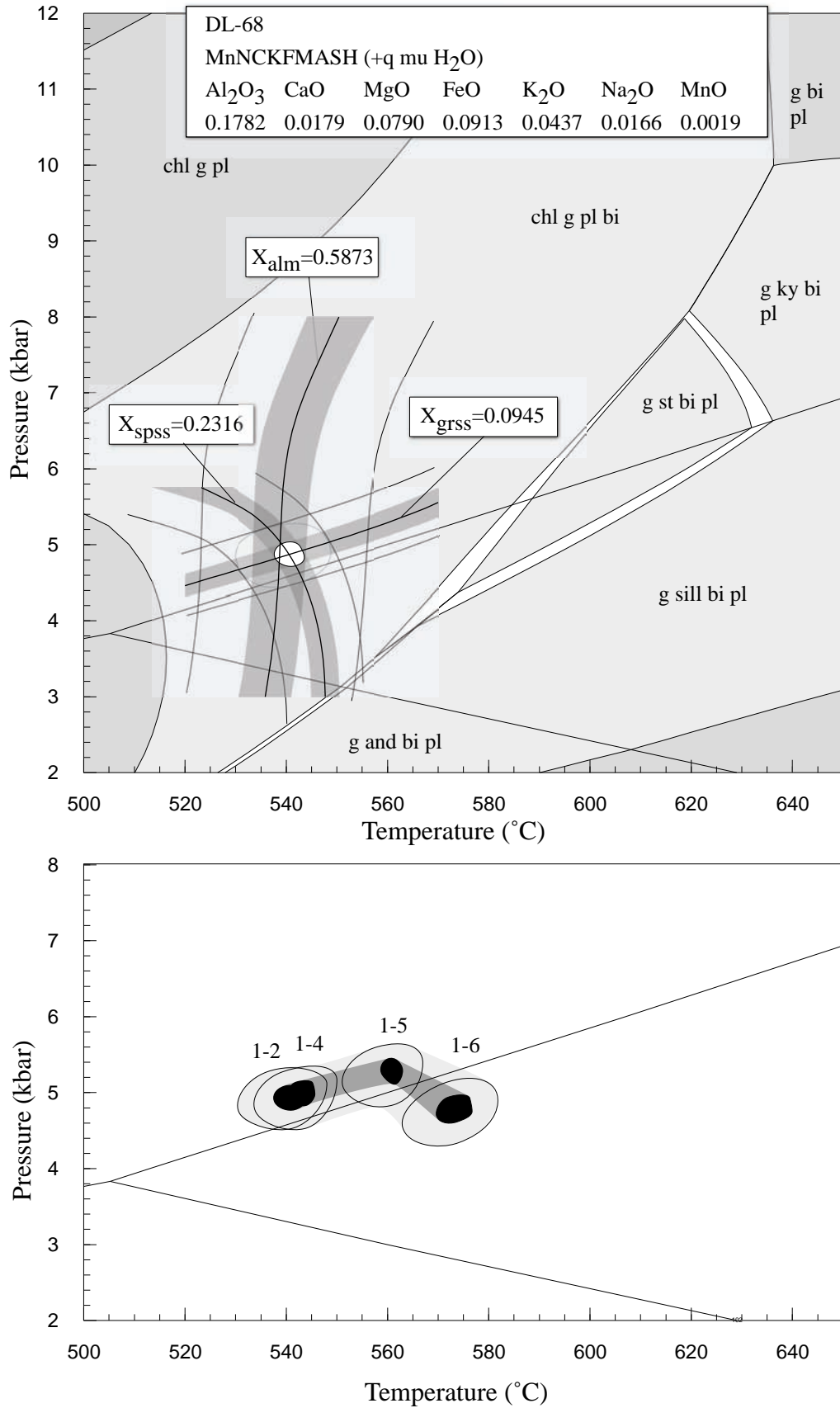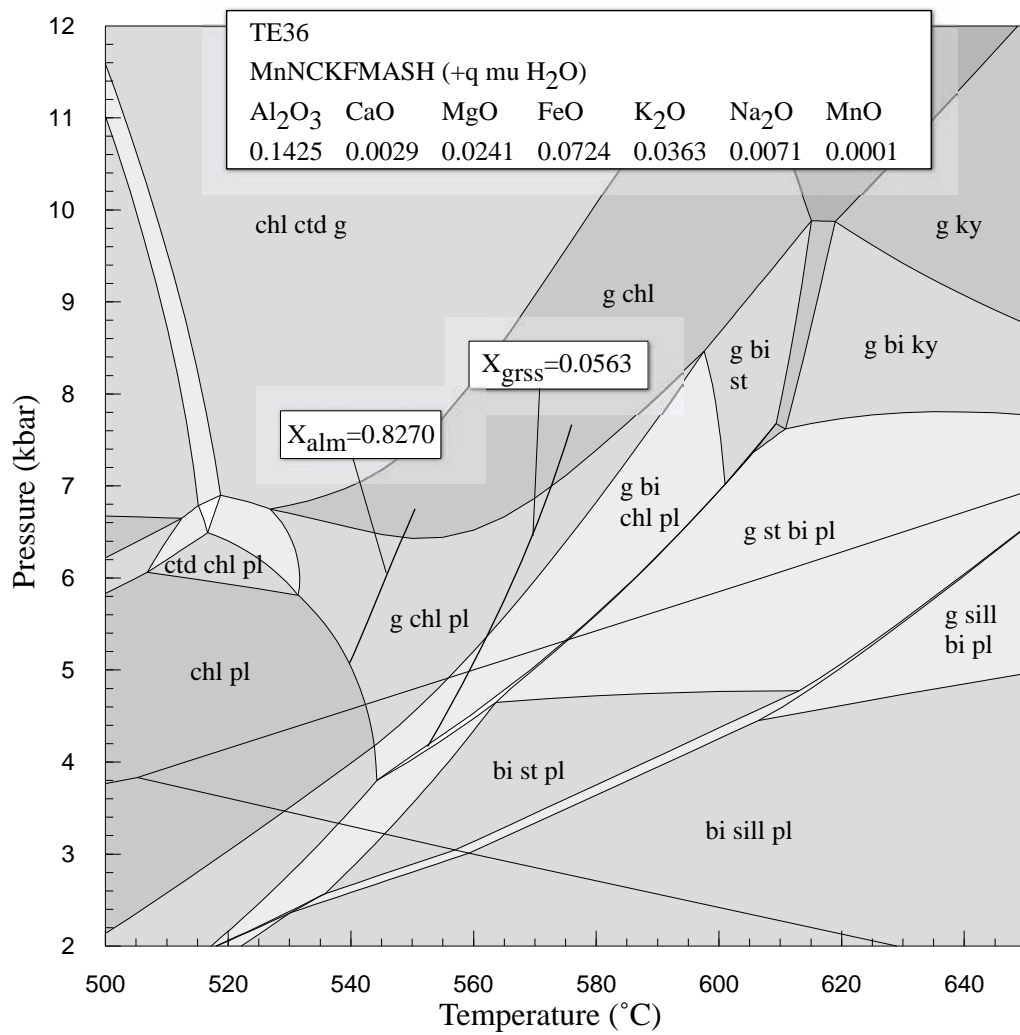
Figure 13. (a) Pseudosection and garnet core isopleths calculated for sample DL-68. **(b)** Core to rim isopleth intersection ellipses calculated with respect to a fractionating bulk composition

Figure 14. (a) Pseudosection and garnet core isopleths calculated for sample TE19. **(b)** Core to rim isopleth intersection ellipses calculated with respect to a fractionating bulk composition

Figure 15. (a) Pseudosection and garnet core isopleths calculated for sample TE21. **(b)** Core to rim isopleth intersection ellipses calculated with respect to a fractionating bulk composition

Figure 16. (a) Pseudosection and garnet core isopleths calculated for sample TE35. **(b)** Core to rim isopleth intersection ellipses calculated with respect to a fractionating bulk composition

Figure 17. Pseudosection and garnet core isopleths for sample TE36. The bulk composition and compositional isopleths are quoted as mol fractions.
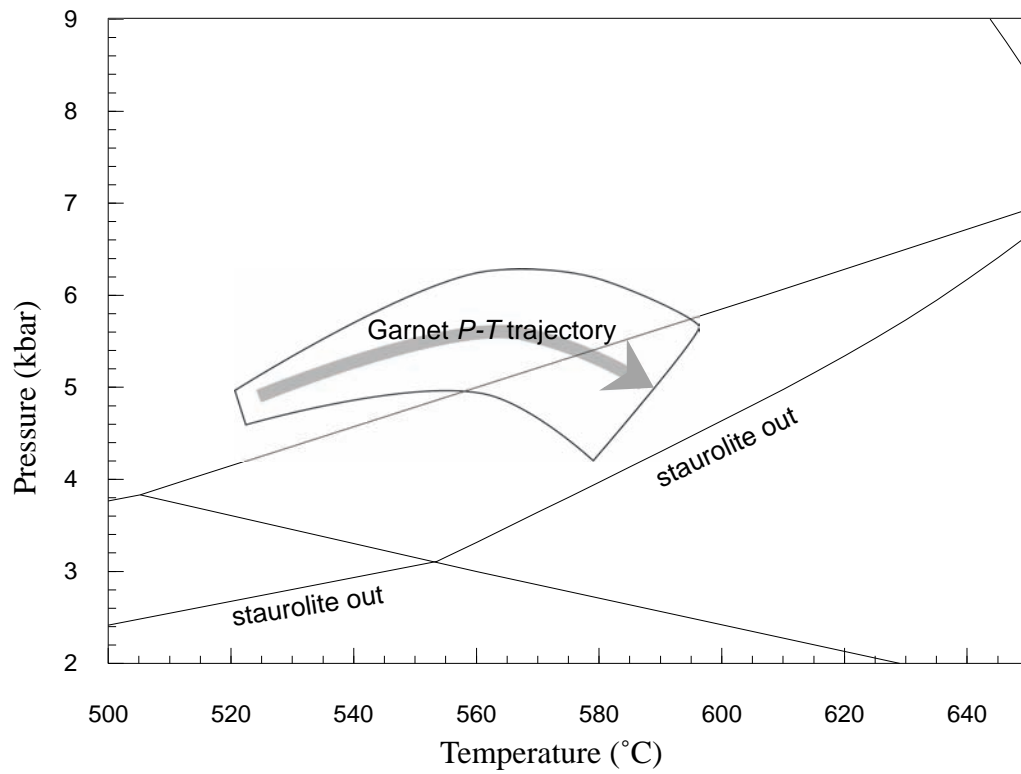
Figure 18. Generalised *P-T* path from garnet compositions from all samples modelled. The staurolite-out line provides an upper limit on peak metamorphic conditions.
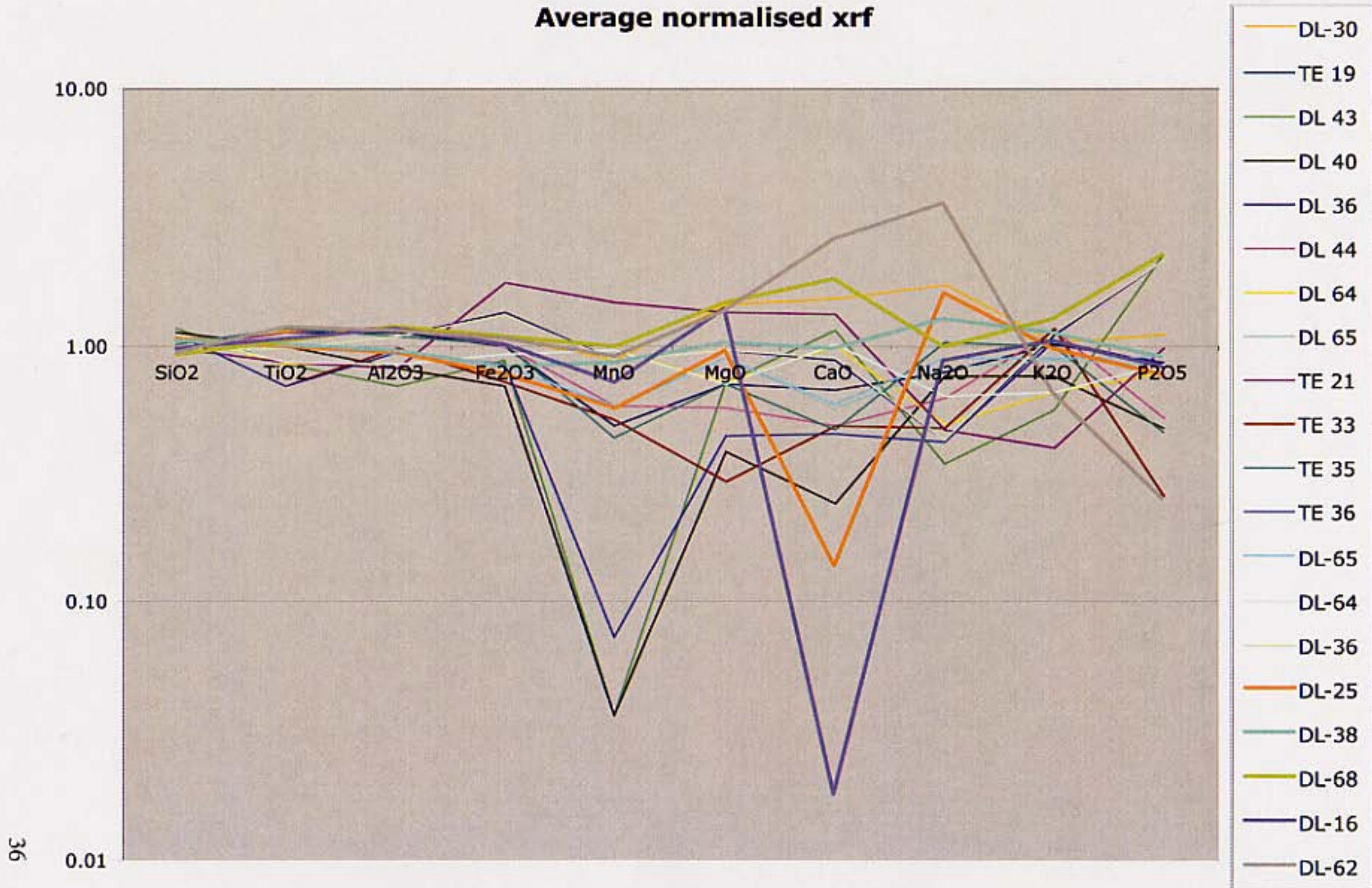
Figure 19. Plots of all XRF results for Littleton formation normalised to the mean of all results